



HAL
open science

Core-Cross-Linked Micelles Made by RAFT Polymerization with a Polycationic Outer Shell Based on Poly(1-methyl-4-vinylpyridinium)

Hui Wang, Lorenzo Vendrame, Christophe Fliedel, Si Chen, Eric Manoury,
Xuewei Zhang, Franck D'agosto, Muriel Lansalot, Rinaldo Poli

► **To cite this version:**

Hui Wang, Lorenzo Vendrame, Christophe Fliedel, Si Chen, Eric Manoury, et al.. Core-Cross-Linked Micelles Made by RAFT Polymerization with a Polycationic Outer Shell Based on Poly(1-methyl-4-vinylpyridinium). *Macromolecules*, 2020, 53 (6), pp.2198-2208. 10.1021/acs.macromol.9b02582 . hal-02611581

HAL Id: hal-02611581

<https://hal.science/hal-02611581>

Submitted on 30 Oct 2020

HAL is a multi-disciplinary open access archive for the deposit and dissemination of scientific research documents, whether they are published or not. The documents may come from teaching and research institutions in France or abroad, or from public or private research centers.

L'archive ouverte pluridisciplinaire **HAL**, est destinée au dépôt et à la diffusion de documents scientifiques de niveau recherche, publiés ou non, émanant des établissements d'enseignement et de recherche français ou étrangers, des laboratoires publics ou privés.

Core-cross-linked micelles made by RAFT polymerization with a polycationic outer shell based on poly(1-methyl-4-vinylpyridinium)

Hui Wang,^a Lorenzo Vendrame,^a Christophe Fliedel,^a Si Chen,^a Florence Gayet,^a Eric Manoury,^a Xuewei Zhang,^b Franck D'Agosto,^b Muriel Lansalot,^b Rinaldo Poli*^{ac}.

^a CNRS, LCC (Laboratoire de Chimie de Coordination), Université de Toulouse, UPS, INPT, 205 route de Narbonne, BP 44099, F-31077 Toulouse Cedex 4, France. ^b Univ Lyon, Université Claude Bernard Lyon 1, CPE Lyon, CNRS, UMR 5265, Chemistry, Catalysis, Polymers and Processes (C2P2), 43 Bd du 11 Novembre 1918, 69616 Villeurbanne, France. ^c Institut Universitaire de France, 1, rue Descartes, 75231 Paris Cedex 05, France.

KEYWORDS. Amphiphilic block copolymer. Polyelectrolyte. RAFT polymerization. Polymerization-induced self-assembly. Poly(1-methyl-4-vinylpyridinium iodide). Core-cross-linked micelle. Nanogel.

ABSTRACT: A convergent synthesis of amphiphilic polymers with a polystyrene (PS) core and a polyelectrolytic poly(1-methyl-4-vinylpyridinium iodide) (P4VPMe⁺I) shell is reported. The polymers were obtained by reversible addition-fragmentation chain-transfer (RAFT) polymerization in water using a trithiocarbonate chain transfer agent [R₀-SC(S)SPr, R₀ = -C(Me)(CN)CH₂CH₂-COOH]. Two types of particle structure, both having spherical morphology and diameters in the 85-150 nm range, have been obtained as stable latexes with polymer content up to 10% in weight. The first structure consists of core-cross-linked micelles (CCMs), where amphiphilic P4VPMe⁺I-*b*-PS arms are cross-linked at the hydrophobic end by the use of diethylene glycol dimethacrylate (DEGDMA). The Coulombic repulsion between the outer shells of the precursor micelles ensures the absence of macrogelation during the cross-linking step. The second structure consists of nanogels (NGs), where the entire hydrophobic core is cross-linked during the last step of simultaneous chain extension and cross-linking of a P4VPMe⁺I-*b*-PS intermediate with a short PS block. The lack of radical polymerization for the 4VPMe⁺I monomer and the lack of chain extension with styrene for a R₀-P4VPMe⁺I-SC(S)SPr intermediate were circumvented by the synthesis of R₀-P4VP-*b*-PS-SC(S)SPr containing a short PS block by sequential RAFT polymerization of 4-vinylpyridine (4VP) and styrene, followed by quantitative cationization of the P4VP block by MeI, and subsequent sequential (for the CCMs) or simultaneous (for the NGs) chain extension and cross-linking.

Introduction

We have recently started a research program aimed at developing polymeric platforms for aqueous biphasic catalysis,¹ which is an attractive protocol to transform hydrophobic substrates into hydrophobic products. In biphasic catalysis, the catalyst is confined in a liquid phase different from that of the reactants/products (*e.g.* water in the aqueous biphasic protocol) and separation at the end of the transformation is readily accomplished by decantation. The process can function in four distinct ways: (i) homogeneous in the catalyst phase if the substrates are sufficiently water-soluble; (ii) homogeneous in the substrate/product phase when the catalyst is sufficiently soluble in the substrate phase or can be transported there by a temperature stimulus or by a phase transfer agents; (iii) heterogeneous (interfacial) when neither component is sufficiently soluble in the other component phase; (iv) homogeneous within nanoreactors, held as a stable dispersion in a phase different from that of the substrates/products. The latter is the operational mode that has attracted our attention. In this protocol,^{2,3} the catalyst is typically confined within the hydrophobic core of self-assembled amphiphilic diblock copolymer micelles, in which the substrate is compatible. However, such micelles suffer from equilibrium with the free arms, leading to catalyst loss at the liquid-liquid interface and as inverse micelles in the substrate/product phase, as well as from extensive swelling, which may lead to stable emulsions and slower decantation. In that spirit, we have introduced two new types of unimolecular amphiphilic core-shell

polymeric particles with a ligand-functionalized hydrophobic core and a hydrophilic shell. The first type contains amphiphilic diblock copolymers with all arms tied together at the hydrophobic chain-end (core-cross-linked micelles, or CCMs)^{4,5} while the second one has a fully cross-linked and functionalized nanogel core, decorated with linear hydrophilic chains in the outer shell (nanogels or NGs).⁶ Other types of unimolecular polymer-based catalytic nanoreactors have been developed,⁷⁻¹⁰ though they were not employed under aqueous biphasic conditions. Our catalytic nanoreactors were built by reversible addition-fragmentation chain transfer (RAFT) polymerization, using the “polymerization-induced self-assembly” (PISA) operating conditions.¹¹⁻¹⁴ They contain a polystyrene (PS) core with anchored ligands (*e.g.* triphenylphosphine or bis(*p*-methoxyphenyl)phenylphosphine), a neutral hydrophilic shell based on randomly copolymerized methacrylic acid (MAA) and poly(ethylene oxide) methyl ether methacrylate (PEOMA), and were cross-linked via the use of diethylene glycol dimethacrylate (DEGDMA). Their efficiency, after metal coordination, was demonstrated in the aqueous biphasic rhodium-catalyzed hydroformylation of a model water insoluble α -olefin (1-octene)^{4,6,15,16} and in the rhodium-catalyzed hydrogenation of 1-octene and styrene.¹⁷

In spite of their remarkable efficiency in catalysis, these nanoreactors still suffered from non-negligible losses in the organic product phase and from slow decantation. These phenom-

ena were shown to result from the high-temperature lipophilicity of the neutral P(MAA-*co*-PEOMA) shell and from particle aggregation. The latter is the consequence of particle interpenetration.¹⁸ In order to correct these problems, we have envisaged to modify the polymer scaffold by replacing the neutral hydrophilic shell with a polyelectrolytic one. Several previous examples of crosslinked polymer particles with a polyionic outer shell have been described, mostly developed for applications in drug delivery.^{19–25} In this contribution, we describe the synthesis of the first example of a polyelectrolytic-shell CCM nanoreactors with a hydrophobic polystyrene core and a polycationic shell based on quaternized (methylated) 4-vinylpyridine (4VP) units, $-\text{[CH}_2\text{-CH(4-C}_5\text{H}_4\text{NMe}^+\text{)]-}$ (4VPMe⁺I). In order to optimize the synthesis of these new objects, we have first developed polymers with non-functionalized PS chains in the hydrophobic core. We shall describe the difficulties encountered to reach the target structure using exclusively PISA and present an alternative strategy, which combines PISA in a first step to generate short amphiphilic block copolymers P4VP-*b*-PS, cationization by methylation of the hydrophilic segment, followed by redispersion in water of the resulting block copolymers (P4VPMe⁺I-*b*-PS) for further styrene emulsion polymerization and final cross-linking. As a further point of novelty, the present contribution shows that thanks to the charged nature of the outer shell, the cross-linking step does not require dilution of the cross-linker with styrene to successfully produce well-defined nanoreactors, whereas this was necessary for the synthesis of equivalent CCM particles with a neutral outer shell.⁴ On the basis of this optimized procedure, the synthesis of equivalent core-functionalized polymers for application in biphasic catalysis becomes now possible. That work, currently in progress, will be presented in a forthcoming contribution.

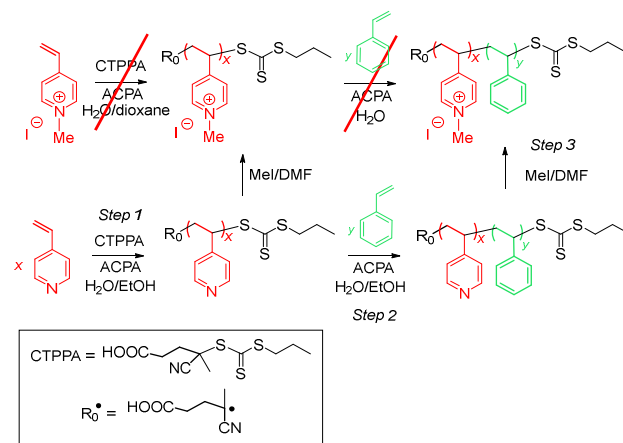
Results and Discussion

For convenience, the formulas of all polymers synthesized in this work and reference to their characterization data is collected in the SI (Table S1).

(a) Preliminary optimization studies

The successful polymer synthesis required removing a few bottlenecks, see Scheme 1. Under conditions identical to those previously optimized for the CCM with the neutral P(MAA-*co*-PEOMA) shell, namely using 4-cyano-4-thiothiopropylsulfanyl pentanoic acid (CTPPA) as RAFT agent and 4,4'-azobis(4-cyanopentanoic acid) (ACPA) as radical initiator, initial attempts were made to directly obtain a hydrosoluble $\text{R}_0\text{-(4VPMe}^+\text{I)}_n\text{-SC(S)SPr}$ macroRAFT agent ($\text{R}_0 = \text{-C(Me)(CN)CH}_2\text{CH}_2\text{-COOH}$) by polymerization of 1-methyl-4-vinylpyridinium iodide, $\text{CH}_2=\text{CH-4-C}_5\text{H}_4\text{NMe}^+\text{I}$ (the experimental details are in the SI). This polymerization was, however, unsuccessful. In a control experiment, we did not observe any polymerization of the same monomer with ACPA initiation under the same operating conditions or with AIBN in a 1:2 dioxane-water solution. In this respect, we note that vinylpyridinium monomers can undergo free radical polymerization,^{27–30} but the kinetic behavior is peculiar with a high reaction order in monomer (e.g. 2.7)²⁷ and thus the polymerization is too slow in dilute solutions. Poly(vinylpyridinium) polymers have also been obtained by free radical polymerization of vinylpyridine, followed by quaternization.^{31, 32} The RAFT polymerization of a vinylpyridinium salt has apparently never been reported, although it has been shown that a controlled RAFT polymerization takes place for other cationic monomers, for instance a styrene containing

a benzylic pyridium substituent in the *para* position, $\text{CH}_2=\text{CH-C}_6\text{H}_4\text{-4-CH}_2\text{C}_5\text{H}_5\text{N}^+\text{Cl}^-$.³³ Additional control experiments have shown the absence of reactivity between the RAFT agent and the monomer, as well as between the RAFT agent and MeI.



Scheme 1. Synthesis of the $\text{R}_0\text{-(4VPMe}^+\text{I)}_x\text{-b-PS}_y\text{-SC(S)SPr}$ diblock copolymer.

In order to overcome this obstacle, the first step of the synthesis was then turned into a RAFT polymerization of neutral 4VP, which required using a water/ethanol mixture in order to keep the system homogeneous and maintain good conditions for further PISA. The RAFT polymerization of 4VP has already been reported in the literature in bulk,³⁴ toluene/ethanol mixture,³⁵ isopropanol,^{36, 37} ethanol³⁸ and THF,³⁹ but to the best of our knowledge never in a water/ethanol mixture. We carried it out in 70/30 (v/v) water/ethanol at 70 °C, initially targeting a low degree of polymerization (Step 1 in Scheme 1 with $x = 60$). The polymerization proceeded to a 93% monomer consumption and the resulting $\text{R}_0\text{-4VP}_{56}\text{-SC(S)SPr}$ product shows a narrow molar mass distribution ($\mathcal{D} = 1.09$) with $M_n = 5800$ g mol⁻¹ (vs. a theoretical value of 6100 g mol⁻¹), indicating good control. The conversion vs. time curve and SEC analysis are available in the SI (Figure S1) and the NMR spectrum of the final solution is shown in Figure 1a.

Full quaternization of the P4VP block in this polymer was then accomplished by reaction with excess MeI in dimethylformamide (DMF) to yield $\text{R}_0\text{-(4VPMe}^+\text{I)}_{56}\text{-SC(S)SPr}$, aiming at a direct chain extension with a polystyrene block. The product was obtained as a solid after removing DMF by dialysis against pure water and freeze-drying. This procedure also removed the water-soluble $\text{Me}_2\text{NH}_2^+\text{I}^-$ co-product, the formation of which was evidenced by a later NMR study (*vide infra*). The ¹H NMR spectrum of the isolated $\text{R}_0\text{-(4VPMe}^+\text{I)}_{56}\text{-SC(S)SPr}$ in DMSO-*d*₆ (Figure 1b) shows that the ¹H NMR resonances of the P4VP aromatic CH protons at δ 8.21 and 6.55 have been fully replaced by those of the $-\text{C}_5\text{H}_4\text{NMe}^+$ rings of the P4VPMe⁺I block at δ 8.77 and ca. 8 (br), plus the Me resonance at δ 4.2. After redispersion in water, a chain extension with styrene was attempted. However, after 3h at 80 °C in the presence of ACPA the conversion was very low (< 5%) and no latex was formed. Prolonging the reaction overnight did not lead to higher conversions. A possible rationalization of the lack of chain extension is based on the charged nature of the macroRAFT agent. As already mentioned in the literature,^{40–42} the charged nature of the macroRAFT may disturb the first addition–fragmentation steps,

although successful chain extensions by RAFT-PISA were reported for quaternized poly(2-(dimethylamino)ethyl methacrylate) with 2-hydroxypropyl methacrylate^{43,44} and for poly(imidazolium-substituted methacrylate) with 2-vinylpyridine.⁴⁵

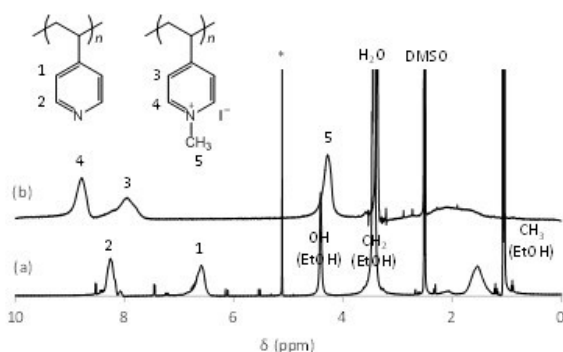


Figure 1. ¹H NMR spectra in DMSO-*d*₆ of (a) R₀-4VP₅₆-SC(S)Pr at the end of the polymerization and (b) isolated R₀-(4VPMe⁺I)₅₆-SC(S)SPr macroRAFT. In spectrum (a), the methylene resonance of the ethanol co-solvent overlaps with the stronger water resonance and the starred resonance is the trioxane internal standard used to monitor the monomer conversion.

In order to circumvent this new obstacle, the direct chain extension of R₀-4VP₅₆-SC(S)SPr with a PS block was then carried out before methylation. In this respect, the literature shows the use of the same strategy, using nitroxide mediated polymerization (NMP), to synthesize a related diblock copolymer, P(4VP⁺Br⁻)-*b*-PDMAA: initial 4VP polymerization, followed by extension with DMAA and final quaternization of the P4VP block pyridine rings by RBr.⁴⁶ The RAFT method has previously been used to generate PS-*b*-P4VP polymers by sequential monomer addition by extending a PS macroRAFT chain with a P4VP block in a variety of solvents (DMF,^{47,48} MeOH,⁴⁹ CO₂/isopropanol³⁷) or in bulk⁵⁰, and also by extending a P4VP macroRAFT with a PS block in methanol⁵¹ or methanol/water⁵² involving PISA. Starting with the R₀-4VP₅₆-SC(S)SPr macroRAFT agent leads to the formation of a R₀-4VP₅₆-*b*-S₂₄₇-SC(S)SPr product with $\bar{D} = 1.1$ for $M_n = 35500 \text{ g mol}^{-1}$, vs. a theoretical molar mass of 32000 g mol^{-1} (see experimental details in the SI). The conversion as a function of time (Figure S2a) is characterized by an induction time, typical of PISA, as in the previously developed CCM with the neutral P(MAA-*co*-PEOMA) shell.⁴ After 2 h, the conversion already reached a maximal value (~82%), and a stable latex was obtained. The SEC traces (Figure S2b) illustrate a good control of the polymerization, while dynamic light scattering (DLS) revealed the formation of particles with a diameter around $D_z = 38 \text{ nm}$ and narrow size distribution (PDI = 0.09), see Figure 2a. The particle morphology was observed by transmission electronic microscopy (TEM, Figure 2b), indicating the formation of small spherical particles, consistent with the DLS analysis. It is worth mentioning here that the non-quantitative conversion of 4VP in the first step (93%) is not an impediment for a successful self-assembly during the PS block growth.

The third step of the polymer synthesis was the methylation of the P4VP block by MeI. For this purpose, a polymer with slightly different block molar mass was initially used, R₀-4VP₁₃₇-*b*-S₃₄₄-SC(S)SPr, because this block molar mass would be suitable for generating spherical particles by direct cross-

linking according to our previous studies on the neutral polymers.⁴ The kinetic monitoring and characterization data of this polymer are in the SI, Figures S3-6. The DLS of this sample (Figure S6) shows slightly larger average size and dispersity ($D_z = 63 \text{ nm}$, PDI = 0.39) than the equivalent polymer with shorter blocks, with evidence of a certain degree of agglomeration, which is confirmed by the TEM analysis (Figure S6). The methylation step was accomplished by addition of a DMF solution of MeI to the P4VP-*b*-PS latex in the H₂O/EtOH mixture. The ¹H NMR monitoring before polymer isolation not only confirmed the quantitative methylation, but also revealed the formation of a significant amount of Me₂NH₂⁺, identified by the NMR resonances at $\delta 2.56$ (CH₃, t, J = 5.6 Hz) and 8.16 (NH₂, broad), and HCOOH, identified by a sharp resonance at $\delta 8.10$ (see the NMR characterization in Figures S7 and S8) and confirmed by control experiments (see Figure S9). This product forms because of the simultaneous presence of DMF, water and MeI (see the proposed mechanism in Scheme S1).⁵³ Solvent removal by vacuum filtration (leading to a viscous residue), followed by thorough washing with water to completely remove the dimethylammonium salt by-product and final vacuum drying, led to a gummy and sticky final product in relatively low yields, which retained DMF (24 molecules per chain according to NMR integration) and variable amounts of water. The DLS ($D_z = 236 \text{ nm}$, PDI = 0.13) and TEM analyses of the isolated and cleaned polymer after redispersion in water (see Figure 3), demonstrate the regular spherical shape and relatively narrow size dispersity for the self-organized diblock R₀-(4VPMe⁺I)₁₃₇-*b*-S₃₄₄-SC(S)SPr chains. The very large increase in the particle size upon cationization may not only be attributed to the much better solvated outer shell in the aqueous solvent but also to the formation of aggregates upon redispersion, entrapping block copolymer chains. Although the DLS and TEM characterization suggest that this product might be suitable for further macromolecular synthesis by cross-linking, its poorly tractable nature and the low yields led us to develop an alternative, optimized procedure, as described in the next section.

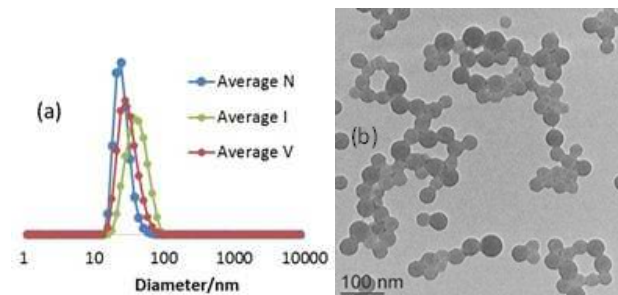


Figure 2. DLS (a, unfiltered sample) and TEM (b) characterization for the (R₀-4VP₅₆-*b*-S₂₄₇-SC(S)SPr) latex.

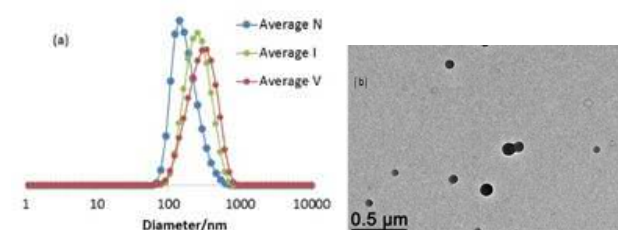


Figure 3. DLS (a, unfiltered sample) and TEM (b) characterization of the [R₀-(4VPMe⁺I)₁₃₇-*b*-S₃₄₄-SC(S)SPr]·24(DMF) latex.

(b) Optimized synthesis and characterization of the amphiphilic P4VPMe⁺I-*b*-PS macroRAFT latex

Because of the above mentioned difficulties in handling the R₀-4VP₁₃₇-*b*-S₃₄₄-SC(S)SPr product, the final strategy consisted in methylation of a P4VP-*b*-PS diblock with a shorter polystyrene block (DP = 50), sufficient to induce micelle formation, followed by cationization of the P4VP block and then further chain extension with a longer PS chain. Incidentally, this allows additional flexibility for the potential synthesis of other objects, such as ligand-functionalized cores,^{4, 16} or nanogel core⁶ architectures, which indeed correspond to the final targets of our research efforts. The same macroRAFT agent of average formula R₀-4VP₁₃₇-SC(S)SPr, used in the above optimization studies, was extended in step 2 (Scheme 1) with a short PS block to obtain R₀-4VP₁₃₇-*b*-S₄₈-SC(S)SPr. The SEC monitoring showed the expected molar mass increase (Figure S10) in fair agreement with the calculated values, while the dispersity remained low (1.25) and the ¹H NMR monitoring (Figure S11) confirmed the nearly complete monomer consumption. In addition, the DOSY NMR spectrum (Figure S12) confirmed that all polymer signals, notably the aromatic CH signals of both pyridine and phenyl rings, correspond to a single diffusion coefficient. The DLS and TEM analyses (Figure S13) show a relatively narrow distribution with D_z = 24.4 nm and PDI = 0.14, though containing a few large agglomerates, and particles with a spherical morphology, respectively.

The cationization with MeI in DMF in step 3 proceeded as smoothly as for the diblock copolymer with the longer PS block (see above). In this case, however, the final polymer extensively precipitated and could be efficiently separated from the liquid phase by centrifugation. Since the Me₂NH₂⁺ salt by-product is quite soluble in DMF, it could be fully eliminated from the isolated polymer (Figure S14) by repetitive washings, followed by a final solvent change to diethyl ether and drying. The global yield of the cationization step after several washings was 67%. Integration of the ¹H NMR spectrum (Figure S15) indicates that the isolated material retains a significant amount of DMF, [R₀-(4VPMe⁺I)₁₃₇-*b*-S₄₈-SC(S)SPr]·38(DMF). This copolymer was then redispersed in water for further chain extension. After redispersion in water, the resulting dispersion showed the presence of large agglomerates and a broad size distribution in DLS, with D_z = 276 nm and PDI = 0.25 (see Figure S16a), whereas dispersion in a water-ethanol (75:25) mixture gave particles of much smaller average size (D_z = 30.0 nm and PDI = 0.48), though still containing large agglomerates (Figure S16b). This could indicate the formation of large compound micelles that trap a certain number of R₀-(4VPMe⁺I)₁₃₇-*b*-S₄₈-SC(S)SPr block copolymer micelles into aggregates.⁵⁴ However, this did not hamper the use of this macroRAFT intermediate to ultimately generate unimolecular polymeric nanoparticles of small size and narrow size distribution (*vide infra*).

Further chain extension in water of R₀-(4VPMe⁺I)₁₃₇-*b*-S₄₈-SC(S)SPr in a fourth step with additional styrene (297 equiv. per chain) resulted in nearly total styrene incorporation (see monitoring in Figure S17) and formation of a stable latex with small size individual particles (D_z = 115.9 nm, PDI = 0.06, Figure S18a). The TEM analysis also confirmed the spherical morphology and narrow size distribution of the polymer micelles (Figure S18b). The narrowness of the particle size distribution and the lower particle size obtained after polymerization are good indications that the chain extension was successful and

that a R₀-(4VPMe⁺I)₁₃₇-*b*-S₄₈-*b*-S₂₉₇-SC(S)SPr block copolymer was obtained. In all evidence, extension of the amphiphilic diblock PS chains results in a breakdown of the large aggregates and in a reorganization in the form of spherical micelles. These micelles are kinetically quite stable, since addition of toluene and vigorous stirring of the latex at room temperature led to neither excessive swelling nor to the formation of emulsions, as shown by DLS (Figure S19a,b). Prolonged heating at 80 °C led to micelle reorganization with formation of smaller objects for the unswollen micelles, and to significant expansion for the swollen ones (Figure S19c,d).

Searching for a compatibilizing solvent for the two blocks, the polymer was freeze-dried and redispersed in DMSO, yielding again micelles (D_z = 43.8 nm, PDI = 0.22, Figure S20a). This micellar structure was maintained, though some agglomeration occurred, after heating the dispersion for 24 h at 90 °C (D_z = 96.2 nm, PDI = 0.42, Figure S20b). A variable-temperature DLS study showed a steady D_z decrease as the temperature was increased (Figure 20c), while the size distribution remained monomodal. The smaller size of these micelles relative to those in the water dispersion may be attributed to a poorer solvation of the PVPMe⁺I by DMSO and/or to a lower aggregation number in this medium. The addition of increasing amounts of toluene, which is a good solvent for the PS core and is fully miscible with DMSO, maintained a stable dispersion up to 40% (v/v), whereas greater toluene fractions led to polymer precipitation. Incidentally, the precipitated polymer showed the same PVPMe⁺/PS ratio as the freeze-dried residue in the ¹H NMR spectrum, whereas no detectable polymer resonances were found in the mother liquor, indicating the absence of PS homopolymer chains. The DLS analyses of the dispersions obtained at variable DMSO/toluene ratios at room temperature (Figure 4) suggested a progressive disaggregation of the micelles and an equilibrium with free chains as the toluene fraction increased. The DMSO/toluene 60:40 (v/v) mixture appears able to solvate both blocks, without polymer precipitation, though an equilibrium is already visible with an 80:20 mixed solvent at room temperature. Finally, the freeze-dried sample redispersed in the 80:20 DMSO/toluene mixture was heated for 24 h at 90 °C. In this case, the DLS analysis of the resulting dispersion showed a trimodal distribution suggesting the presence of micelles, middle-size nanoaggregates and much larger particles stabilized by the diblock copolymer (Figure S21b).

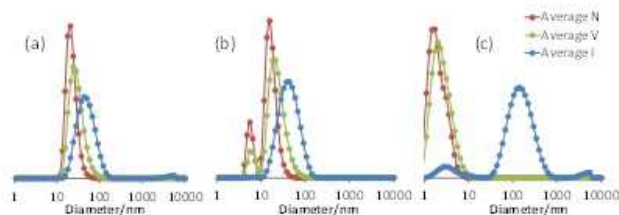
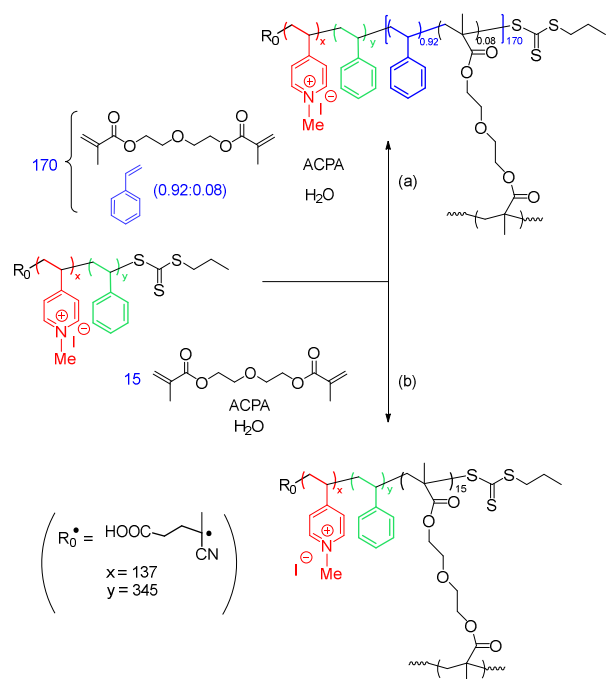


Figure 4. DLS of R₀-(4VPMe⁺I)₁₃₇-*b*-S₄₈-*b*-S₂₉₇-SC(S)SPr after freeze-drying the aqueous latex and redispersion in (a) neat DMSO; (b) DMSO/toluene 80:20; (c) DMSO/toluene 60:40 (unfiltered samples).

(c) Cross-linking of the amphiphilic P4VPMe⁺I-*b*-PS copolymer with high molar mass PS block

The particles resulting from the synthesis outlined above, henceforth written as R₀-(4VPMe⁺I)₁₃₇-*b*-S₃₄₅-SC(S)SPr, were first cross-linked according to the previously published protocol,⁴ which made use of a DEGDMA/styrene mixture. Dilution

of the DEGDMA cross-linker with a large amount of styrene was found necessary, in the previous synthesis of the CCM and NG particles containing the neutral P(MAA-co-PEOMA) hydrophilic shell,^{4, 6} to avoid macrogelation. Application of the same conditions, using a DEGDMA/styrene molar ratio of 7.7:92.3 ratio for a total of 170 equiv per chain (Scheme 2, path (a)), yielded R_0 -(4VPMe⁺I)₁₃₇-*b*-S₃₄₅-*b*-(S₁₅₇-*co*-DEGDMA₁₃)-SC(S)SPr (¹H NMR monitoring in Figure S22), in which each polymer chain has an average molar mass of $9.17 \cdot 10^4$ g mol⁻¹. The NMR spectrum in DMSO-*d*₆/H₂O does not show the PS core, because this solvent mixture is not able to swell it. However, all polymer parts become visible in a colloidal dispersion with the particle core swollen by CDCl₃, see Figure 5.



Scheme 2. Cross-linking step for the synthesis of the CCM with a polycationic P(4VPMe⁺I) shell.

The final latex has once again the aspect of a homogeneous and stable white dispersion. The DLS results (Figure 6a) revealed one population of objects with a narrow size distribution (PDI = 0.09) and an average D_z of 143 nm. The measurement was repeated after stirring the sample with excess toluene, resulting in particle swelling, followed by decantation, yielding $D_z = 156$ nm (PDI = 0.04), Figure 6b. The swelling process was rapid (shaking for < 1 min), as indicated visually by the change of relative volumes, before and after shaking, of the aqueous and organic phases. This demonstrates the feasibility of mass transport for organic molecules compatible with PS toward the particle core. On the basis of a spherical shape (as confirmed by the TEM analysis, Figure 6c) the average volume increase by swelling can be calculated as 29.8% and $\Delta V = (4/3)\pi[(156/2)^3 - (143/2)^3] = 4.57 \cdot 10^5$ nm³. Using the density (0.865 g cm⁻³) and molecular weight (92.14 g mol⁻¹) of toluene and Avogadro's number, this allows to estimate an average of $\approx 2.6 \cdot 10^6$ toluene molecules per swollen particle.

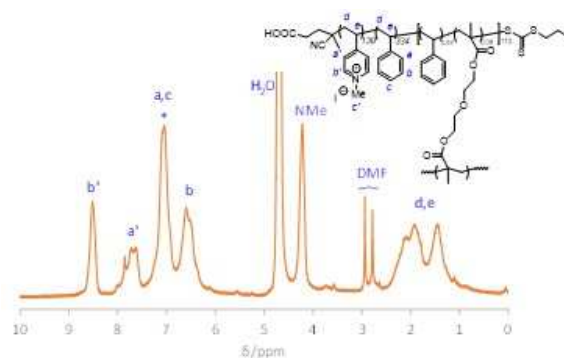


Figure 5. ¹H NMR spectrum of the final CCM R_0 -(4VPMe⁺I)₁₃₇-*b*-S₃₄₅-*b*-(S₁₅₇-*co*-DEGDMA₁₃)-SC(S)SPr swollen by CDCl₃ in H₂O. The starred resonance also contains the residual protons of CDCl₃.

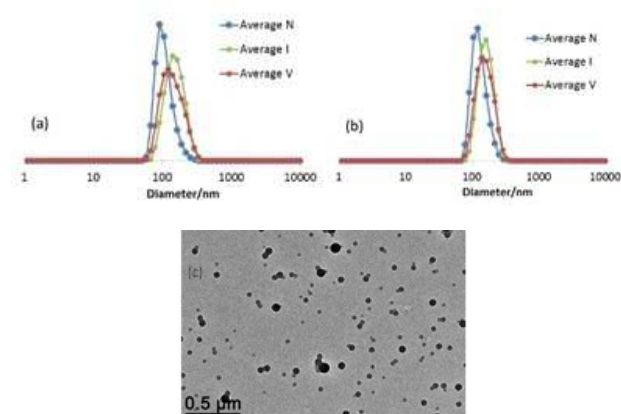


Figure 6. DLS and TEM analyses of the R_0 -(4VPMe⁺I)₁₃₇-*b*-S₃₄₅-*b*-(S₁₅₇-*co*-DEGDMA₁₃)-SC(S)SPr CCM latex. (a) DLS (unfiltered sample, $D_z = 142$ nm, PDI = 0.09). (b) DLS after swelling with toluene (unfiltered sample, $D_z = 156$ nm, PDI = 0.04). (c) TEM image of the final particles.

Several experiments were conducted in order to assess the stability of the CCM scaffold and the extent of the cross-linking step. A latex with a closely related formula from an independent synthesis, (R_0 -(4VPMe⁺I)₁₄₀-*b*-S₃₅₀-*b*-(S₁₄₅-*co*-DEGDMA₁₅)-SC(S)SPr), characterized by a narrow size distribution ($D_z = 110.6$ nm, PDI = 0.19; Figure S23a), was heated for 24 h at 90 °C in order to probe its thermal stability. The treatment gave no evidence of alteration, notably the latex remained a stable colloidal suspension with no sign of coagulation, but the DLS analysis after the treatment revealed slightly smaller particles ($D_z = 89.7$ nm, PDI = 0.10; Figure S23b). This behavior is similar to that observed for the precursor micelles, raising doubts about a possible incomplete cross-linking step, because the contraction may result from reorganization with loss of free arms. On the other hand, a slight contraction may also result from relaxation of the glassy polystyrene core upon prolonged treatment under conditions close to the glass transition temperature. The same thermal treatment was also carried out on the same latex after swelling with toluene: the swollen particles ($D_z = 112.3$, PDI = 0.10, Figure S23c) showed an expansion ($D_z = 254.1$, PDI = 0.24, Figure S23d) after heating for 24 h at 90 °C, in close analogy to the behavior of the precursor diblock arm micelles. Freeze-drying, followed by redispersion in water, gave a size distribution similar as to that of the latex from synthesis, with

no evidence of coagulation ($D_z = 119.0$ nm, PDI = 0.10, Figure 23e).

In order to further probe the possible presence of uncross-linked arms, the freeze-dried polymer was also redispersed in a DMSO/toluene (80/20 v/v) mixture, followed by heating, because this treatment was shown to release single chains from the micelles, as evidenced by the DLS analysis (*vide supra*). However, the dispersion (initial $D_z = 63.0$ nm, PDI = 0.09, Figure S24a) only showed a slight size increase after 24 h at 90 °C ($D_z = 73.1$ nm, PDI = 0.11, Figure S24b) and the absence of a small size distribution attributable to single chains. This results clearly suggests that the core-crosslinking step of the polymer synthesis is essentially quantitative, with an insignificant amount of residual free arms.

The P4VPMe⁺I-*b*-PS-SC(S)SPr macroRAFT chains with the long PS block were also cross-linked in the last step by pure DEGDMA (absence of styrene, Scheme 2, path (b)). The motivation to attempt this synthesis was the previous failure to obtain well-defined spherical CCM particles, when using pure DEGDMA in the last step, in the presence of a neutral P(MAA-*co*-PEOMA) hydrophilic shell.⁴ Rather, such polymerization resulted in the formation of a macrogel. The reason for that behavior was attributed to reversible particle-particle interpenetration, as separately proven by experiments on interparticle metal migration.¹⁸ It was also shown that the metal migration is almost completely stopped after complete deprotonation of the shell carboxylic acid functions with NaOH at high pH, to yield a P(MAA⁻Na⁺-*co*-PEOMA) shell. Furthermore, it was demonstrated that the slow residual metal migration occurs via molecular species through the continuous aqueous phase and not by associative exchange after particle interpenetration. Therefore, MAA deprotonation introduces repulsive Coulombic forces between the different particles, which no longer allow interpenetration. On these grounds, it was of interest to probe whether the analogous inter-particle Coulombic repulsion induced by the positively charged outer shell of our current micelles would allow cross-linking without macrogelation.

For this purpose, a new macroRAFT agent of average formula $R_0-(4VPMe^+I)_{137-b-S_{48}}-SC(S)SPr$ was prepared and converted into $R_0-(4VPMe^+I)_{137-b-S_{345}}-SC(S)SPr$, see Scheme 2(b). The DLS of this polymer (Figure S25) confirmed the expected sample uniformity and size, which did not significantly change after addition of DEGDMA (15 equiv per chain), with D_z changing from 139.1 nm (PDI = 0.11) to 137.3 nm (PDI = 0.11). The cross-linking reaction proceeded rapidly with nearly complete monomer consumption (NMR monitoring, Figure S26) to yield a latex as a stable colloidal suspension, without any evidence of macrogelation. The ¹H NMR spectrum in D₂O of the polymer particles with CDCl₃-swollen core clearly shows all expected resonances (Figure S27), except those of the central DEGDMA cross-linked part, which is not unexpected because these resonances should be low-intensity, overshadowed by the strong water resonance, and probably too broad because of the tight cross-linking (long correlation time). The DLS and TEM analyses (Figure 7) show the absence of agglomerates and confirm the quality of the product as particles with a narrow size distribution. The average size obtained from DLS for these particles ($D_z = 148$ nm; PDI = 0.09 for the unswollen sample and $D_z = 162$ nm; PDI = 0.10 for the toluene-swollen one) is slightly greater than for those obtained when styrene was also used in the cross-linking step. For these particles, the average size increase by swelling is 31.1%, with an average volume increase

of $5.29 \cdot 10^5$ nm³ corresponding to $3.0 \cdot 10^6$ molecules per particle. When compared with the previously published cross-linking, under equivalent conditions, to yield CCM particles with the neutral P(MAA-*co*-PEOMA) hydrophilic shell,⁴ this result demonstrates the positive effect of a charged polycationic shell and of the ensuing Coulombic repulsion to avoid irreversible particle-particle coupling.

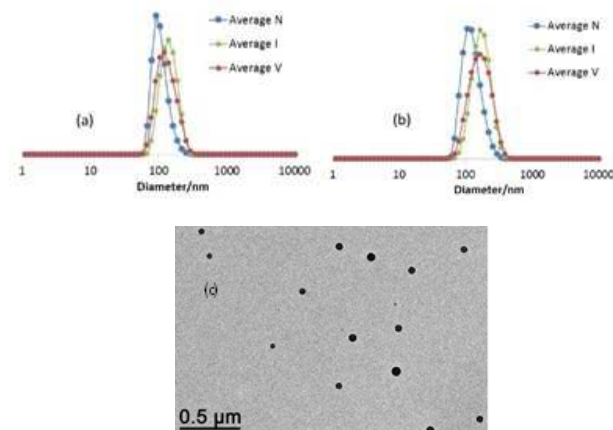


Figure 7. DLS and TEM analyses of the $R_0-(4VPMe^+I)_{137-b-S_{345}}-b-DEGDMA_{15}-SC(S)SPr$ CCM latex. (a) DLS (unfiltered sample). (b) DLS after swelling with toluene (unfiltered sample). (c) TEM image of the final particles.

The same thermal stability, freeze-drying, and redispersion experiments described above for the CCM particles that were cross-linked by the DEGDMA/styrene mixture were also carried out for this new polymer. While the results were quite similar for the aqueous latex (details in Figure S28), heating the freeze-dried and redispersed polymer in a DMSO/toluene (80/20 v/v) mixture for 24 h at 90 °C revealed a significant proportion of free chains (Figure S29). Thus, although the Coulombic screening of the polycationic shell avoids macrogelation and allows using the DEGDMA crosslinker without dilution with styrene, the presence of styrene still appears necessary to ensure a quantitative cross-linking step.

(d) Synthesis of a P4VPMe⁺I-*b*-PS-*b*-P(S-*co*-DEGDMA) nanogel.

As a final synthetic application, the $R_0-(4VPMe^+I)_{137-b-S_{48}}-SC(S)SPr$ macroRAFT intermediate was used for a one-step synthesis of unimolecular polymers with a nanogel core. This was accomplished by copolymerization of styrene and the DEGDMA cross-linker with a P4VPMe⁺I-*b*-PS macroRAFT:S:DEGDMA molar ratio of 1:300:15. The NMR monitoring revealed once again complete monomer conversion (Figure S30), yielding the desired $R_0-(4VPMe^+I)_{137-b-S_{48}}-b-(S_{300-co-DEGDMA_{15}})-SC(S)SPr$. The DLS analysis confirms the generation of uniform particles, although it suggests a minor degree of agglomeration, see Figure S31. The D_z (PDI) is 84.7 nm (0.05) for the unswollen sample, 92.6 nm (0.06) for the CHCl₃-swollen sample (30.7% volume increase; $\Delta V = 9.76 \cdot 10^4$ nm³; $7.3 \cdot 10^5$ molecules per particle), and 88.8 nm (0.06) for the toluene-swollen one (15.2% volume increase; $\Delta V = 4.85 \cdot 10^4$ nm³; $2.7 \cdot 10^5$ molecules per particle). The formation of a few larger agglomerates was however not evident from the TEM analysis (several images were analyzed), which also confirms the presence of individual spherical particles, indicating that the degree of aggregation is very minor (see a representative image in Figure S32). This result, in comparison with the absence of

particle-particle coupling for the CCM syntheses described in the previous sections, shows that the state of aggregation of the diblock precursor is important. The diblock with the long PS chain, *i.e.* $R_0-(4VPMe^+I)_{137}-b-S_{345}-SC(S)SPr$, is pre-organized in the form of individual spherical micelles (Figure S18) and leads to individual particles upon cross-linking, even when using neat cross-linker. On the other hand, the diblock precursor with the short PS chain, *i.e.* $R_0-(4VPMe^+I)_{137}-b-S_{48}-SC(S)SPr$, is self-organized in agglomerated micelles with a broader size distribution (Figure S16) and the cross-linking step consequently leads to the formation of a few particle agglomerates. It is important to underline that in this synthesis, as in all other syntheses described above, all components including the initiator were introduced into the reaction flask before starting to heat the mixture.

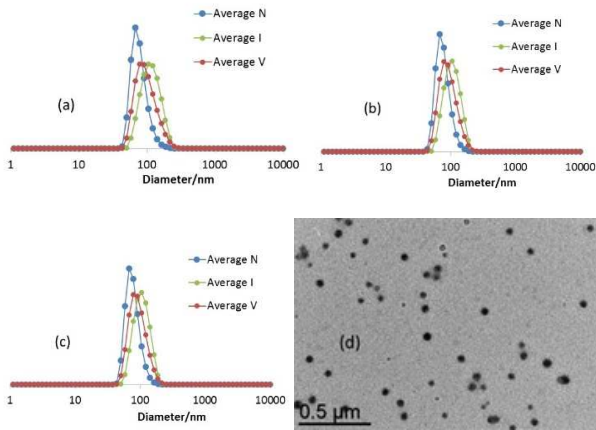


Figure 8. DLS analyses (unfiltered samples) of (a) $R_0-(4VPMe^+I)_{137}-b-S_{48}-SC(S)SPr$ macroRAFT agent after equilibration with styrene (300 equiv) and DEGDMA (15 equiv) in water at 80 °C for 30 min; (b) $R_0-(4VPMe^+I)_{137}-b-S_{48}-b-(S_{300-co-DEGDMA_{15}})-SC(S)SPr$ product; (c) as (b), after swelling with toluene. (d) TEM image of the final product.

Since the results described above clearly demonstrate that the state of aggregation is affected by the hydrophilic/hydrophobic components ratio, notably increasing the hydrophobic fraction favors a breakdown of large aggregates into individual spherical micelles, we reasoned that this nanogel particle synthesis could be improved by first equilibrating the $R_0-(4VPMe^+I)_{137}-b-S_{48}-SC(S)SPr$ macroRAFT agent with all hydrophobic monomers at the reaction temperature in the absence of initiator, before the ACPA addition to start the reaction. Indeed, operating in this way, the initial broad distribution of the $R_0-(4VPMe^+I)_{137}-b-S_{48}-SC(S)SPr$ particles ($D_z = 276$ nm, PDI = 0.25, Figure S16), after monomer addition and equilibration, was transformed into

a narrower distribution of smaller particles ($D_z = 107.0$ nm, PDI = 0.10, Figure 8). Subsequent polymerization yielded a stable colloidal suspension of $R_0-(4VPMe^+I)_{137}-b-S_{48}-b-(S_{300-co-DEGDMA_{15}})-SC(S)SPr$ without any evidence of residual agglomerates by DLS and TEM analyses, see Figure 8. Notably, the size distribution of the final cross-linked polymer particles ($D_z = 101.4$ nm, PDI = 0.06) is relatively close to that of the swollen particles prior to polymerization. The particle size then slightly increased after swelling with toluene ($D_z = 110.5$ nm, PDI = 0.15), corresponding to a 29.4% volume increase ($\Delta V = 1.61 \cdot 10^5$ nm³; $9.1 \cdot 10^5$ molecules per particle). The ¹H NMR spectrum of the particles in D₂O, with the core swollen by CDCl₃, is reported in Figure S33. These particles, like the CCM particles obtained by cross-linking with the DEGDMA-styrene mixture, showed thermal stability, no alteration by freeze-drying and redispersion in water or DMSO, and no evidence of single chain release upon prolonged heating of the freeze-dried polymer redispersed in DMSO/toluene (80:20 v/v) mixture (Figures S34-35).

(a) Zeta potentials.

The zeta potential values, as well as the particle dimensions, measured for all the latexes with a charged shell, before and after cross-linking, are collected in Table 1. All values are, as expected, positive and large, in the same range as those reported for other positively charged polymeric nanoparticles.^{43, 44, 55, 56} The micelles exhibit the highest ζ values, which are not significantly affected by the molar mass of the hydrophobic polystyrene block, but note that these micelles are differently aggregated (*cf.* Figure 3 and Figure S16). The ζ values are slightly reduced for the core-crosslinked micelles and further reduced for the particles with nanogel architecture. However, such changes may not be significant and a rationalization of this trend seems premature at this stage.

Conclusions

In the present paper, we targeted core-cross-linked micelles (CCMs) or nanogels (NGs) with a P4VPMe⁺I polycationic outer shell and a PS core. Our initial approach was based on the use of PISA to chain extend in water a P4VPMe⁺I polymer synthesized by RAFT, with a PS block that could be crosslinked with DEGDMA. However, neither RAFT polymerization of 4VPMe⁺I, nor chain extension in water of a preformed P4VPMe⁺I polymer (obtained after cationization of P4VP synthesized by RAFT) with styrene was successful. This drove us to develop alternative strategies, all relying on the synthesis of P4VP-*b*-PS block copolymer particles obtained by PISA in a mixture of ethanol and water, the stabilizing P4VP layer being post-cationized to provide a P4VPMe⁺I-*b*-PS intermediate.

Table 1. Zeta potentials for selected polymers with polycationic outer shell.

Polymer	Type	ζ/mV	D_z/nm (PDI)
$R_0-(4VPMe^+I)_{137}-b-S_{48}-SC(S)SPr$	Micelle	+45.8	276 (0.25)
$R_0-(4VPMe^+I)_{137}-b-S_{345}-SC(S)SPr$	Micelle	+44.4	139 (0.11)
$R_0-(4VPMe^+I)_{137}-b-S_{345}-b-(S_{157-co-DEGDMA_{13}})-SC(S)SPr$	CCM	+40.8	143 (0.09)
$R_0-(4VPMe^+I)_{137}-b-S_{345}-b-DEGDMA_{15}-SC(S)SPr$	CCM	+40.6	148 (0.09)
$R_0-(4VPMe^+I)_{137}-b-S_{48}-b-(S_{300-co-DEGDMA_{15}})-SC(S)SPr$	NG	+36.1	101 (0.06)

Process optimization to efficiently produce the targeted CCM or NG required a fine tuning of the hydrophilic/hydrophobic balance between the two blocks, with an optimum for short PS block, *i.e.* R₀-4VPMe⁺I₁₃₇-*b*-S₄₈-SC(S)SPr chains that were re-dispersed in water. For the CCM synthesis, these chains were first chain-extended with styrene. Crosslinking successfully took place in a subsequent step using either a mixture of S and DEGDMA or DEGDMA alone. Indeed, in the latter case, particle-particle interpenetration, identified in our previous work⁴ as the main cause of macrogelation, was impeded thanks to the polyelectrolytic nature of the particles. However, the DLS analysis of the particles dispersed in a DMSO/toluene 80:20 (v/v) mixture, which is able to sufficiently solvate both blocks, after prolonged heating showed that a significant amount of uncross-linked, free arms was present when pure DEGDMA was used in the last step. The NGs were obtained by simultaneous chain extension and crosslinking of the R₀-4VPMe⁺I₁₃₇-*b*-S₄₈-SC(S)SPr chains with a mixture of S and DEGDMA. For both CCMs and NGs, positively charged and spherical particles with average D_z in the 85-150 nm range were obtained as stable polymer dispersions, with polymer content up to 10% in weight. Taking advantage of the flexibility of the PISA process, the initially encountered difficulties linked to the charged nature of polyelectrolytic shell were circumvented, leading to the successful formation of the targeted polycationic spherical particles. It has to be mentioned that, while the PISA process has the advantage of producing various ordered structures (including cylindrical micelles and vesicles) by altering the hydrophilic/hydrophobic ratio, the targeted application as nanoreactors for biphasic catalysis would not find any specific advantage in using alternative morphologies relative to spherical particles. These polymers represent a new tool as a support of water-soluble anionic catalysts for application as nanoreactors in interfacial catalysis. Investigations in this direction are ongoing in our laboratories and will be reported in due course. In addition, equivalent particles with ligand-functionalized hydrophobic cores are now accessible by adaptation of the chain extension step that introduces the hydrophobic block. These studies and their applications as nanoreactors in micellar catalysis are also in progress in our laboratories.

ASSOCIATED CONTENT

Supporting Information. Experimental details, NMR spectra, polymerization kinetics, GPC, DLS and TEM characterization of polymer products and intermediates (23 pages). This material is available free of charge via the Internet at <http://pubs.acs.org>.

AUTHOR INFORMATION

Corresponding Author

* Rinaldo Poli. +33-561333174; rinaldo.poli@lcc-toulouse.fr.

Author Contributions

All authors have given approval to the final version of the manuscript.

Funding Sources

Agence Nationale de la Recherche, ANR-11-BS07-025-01 (BIPHASANOCAT).

ACKNOWLEDGMENT

We are grateful to the Centre National de la Recherche Scientifique (CNRS), to the Agence Nationale de la Recherche (project BIPHASANOCAT, grant number ANR-11-BS07-025-01) and to the Institut Universitaire de France (IUF) for financial support. We are also grateful to the China Scholarship Council for a Ph.D. fellowship to HW.

ABBREVIATIONS

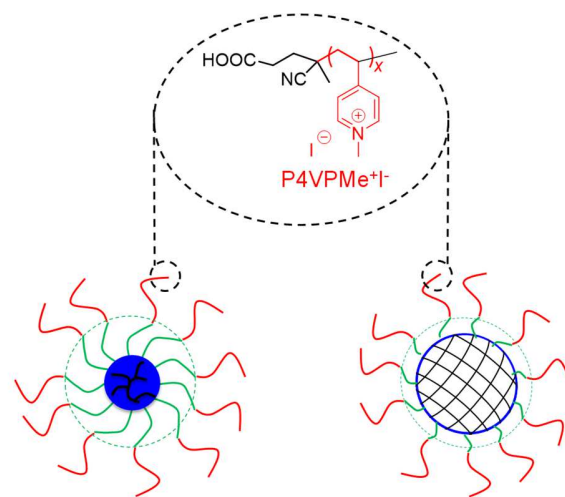
ACPA, 4,4'-azobis(4-cyanopentanoic acid); CCM, core-cross-linked micelle; CTPPA, 4-cyano-4-thiothiopropylsulfanyl pentanoic acid; DEGDMA, diethylene glycol dimethacrylate; DMF, dimethylformamide; MAA, methacrylic acid; NG, nanogel; PISA, polymerization-induced self-assembly; PEOMA, poly(ethylene oxide) methyl ether methacrylate; 4VP, 4-vinylpyridine.

REFERENCES

1. Cornils, B.; Herrmann, W. A., *Aqueous Phase Organometallic Catalysis*. Wiley-VCH: Weinheim, 1997.
2. Cotanda, P.; Petzetakis, N.; O'Reilly, R. K. Catalytic polymeric nanoreactors: more than a solid supported catalyst. *MRS Communications* **2012**, 2 (4), 119-126.
3. Lu, A.; O'Reilly, R. K. Advances in nanoreactor technology using polymeric nanostructures. *Curr. Opin. Biotech.* **2013**, 24 (4), 639-645.
4. Zhang, X.; Cardozo, A. F.; Chen, S.; Zhang, W.; Julcour, C.; Lansalot, M.; Blanco, J.-F.; Gayet, F.; Delmas, H.; Charleux, B.; Manoury, E.; D'Agosto, F.; Poli, R. Core-Shell Nanoreactors for Efficient Aqueous Biphasic Catalysis. *Chem. Eur. J.* **2014**, 20 (47), 15505-15517.
5. Manoury, E.; Gayet, F.; D'Agosto, F.; Lansalot, M.; Delmas, H.; Julcour, C.; Blanco, J.-F.; Barthe, L.; Poli, R., Core-cross-linked micelles and amphiphilic nanogels as unimolecular nanoreactors for micellar-type, metal-based aqueous biphasic catalysis. In *Effects of Nanoconfinement on Catalysis*, Poli, R., Ed. Springer: New York, 2017; pp 147-172.
6. Lobry, E.; Cardozo, A. F.; Barthe, L.; Blanco, J.-F.; Delmas, H.; Chen, S.; Gayet, F.; Zhang, X.; Lansalot, M.; D'Agosto, F.; Poli, R.; Manoury, E.; Julcour, C. Core phosphine-functionalized amphiphilic nanogels as catalytic nanoreactors for aqueous biphasic hydroformylation. *J. Catal.* **2016**, 342, 164-172.
7. Terashima, T.; Kamigaito, M.; Baek, K.-Y.; Ando, T.; Sawamoto, M. Polymer Catalysts from Polymerization Catalysts: Direct Encapsulation of Metal Catalyst into Star Polymer Core during Metal-Catalyzed Living Radical Polymerization. *J. Am. Chem. Soc.* **2003**, 125 (18), 5288-5289.
8. O'Reilly, R. K.; Hawker, C. J.; Wooley, K. L. Cross-linked block copolymer micelles: functional nanostructures of great potential and versatility. *Chem. Soc. Rev.* **2006**, 35 (11), 1068-1083 DOI: 10.1039/b514858h.
9. Liu, Y.; Wang, Y.; Wang, Y. F.; Lu, J.; Pinon, V.; Weck, M. Shell Cross-Linked Micelle-Based Nanoreactors for the Substrate-Selective Hydrolytic Kinetic Resolution of Epoxides. *J. Am. Chem. Soc.* **2011**, 133 (36), 14260-14263.
10. Terashima, T., Polymer Microgels for Catalysis. In *Encyclopedia of Polymer Science and Technology*, 4th Edition, Mark, H. F., Ed. John Wiley & Sons, Inc.: 2013; p 10.1002/0471440264.pst590.
11. Charleux, B.; Delaitre, G.; Rieger, J.; D'Agosto, F. Polymerization-Induced Self-Assembly: From Soluble Macromolecules to Block Copolymer Nano-Objects in One Step. *Macromolecules* **2012**, 45 (17), 6753-6765.
12. Warren, N. J.; Armes, S. P. Polymerization-Induced Self-Assembly of Block Copolymer Nano-objects via RAFT Aqueous Dispersion Polymerization. *J. Am. Chem. Soc.* **2014**, 136 (29), 10174-10185.
13. Canning, S. L.; Smith, G. N.; Armes, S. P. A Critical Appraisal of RAFT-Mediated Polymerization-Induced Self Assembly. *Macromolecules* **2016**, 49 (6), 1985-2001 DOI: 10.1021/acs.macromol.5b02602.

14. D'Agosto, F.; Rieger, J.; Lansalot, M. RAFT-mediated polymerization-induced self-assembly. *Angew. Chem. Int. Ed.* **accepted article**, DOI: 10.1002/anie.201911758.
15. Cardozo, A. F.; Julcour, C.; Barthe, L.; Blanco, J.-F.; Chen, S.; Gayet, F.; Manoury, E.; Zhang, X.; Lansalot, M.; Charleux, B.; D'Agosto, F.; Poli, R.; Delmas, H. Aqueous phase homogeneous catalysis using core-shell nano-reactors: application to rhodium catalyzed hydroformylation of 1-octene. *J. Catal.* **2015**, 324, 1-8.
16. Chen, S.; Cardozo, A. F.; Julcour, C.; Blanco, J.-F.; Barthe, L.; Gayet, F.; Charleux, B.; Lansalot, M.; D'Agosto, F.; Delmas, H.; Manoury, E.; Poli, R. Amphiphilic Core-Cross-linked Micelles functionalized with Bis(4-methoxyphenyl)phenylphosphine as catalytic nanoreactors for biphasic hydroformylation. *Polymer* **2015**, 72, 327-335.
17. Joumaa, A.; Chen, S.; Vincendeau, S.; Gayet, F.; Poli, R.; Manoury, E. Rhodium-catalyzed aqueous biphasic hydrogenation of alkenes with amphiphilic phosphine-containing core-shell polymers. *Mol. Cat.* **2017**, 438, 267-271.
18. Chen, S.; Gayet, F.; Manoury, E.; Joumaa, A.; Lansalot, M.; D'Agosto, F.; Poli, R. Coordination chemistry inside polymeric nanoreactors: interparticle metal exchange processes and ionic compound vectorization in phosphine-functionalized amphiphilic polymer latexes. *Chem. Eur. J.* **2016**, 22, 6302 – 6313.
19. Meng, F. H.; Hennink, W. E.; Zhong, Z. Reduction-sensitive polymers and bioconjugates for biomedical applications. *Biomaterials* **2009**, 30 (12), 2180-2198 DOI: 10.1016/j.biomaterials.2009.01.026.
20. Otsuka, H.; Nagasaki, Y.; Kataoka, K. PEGylated nanoparticles for biological and pharmaceutical applications. *Advanced Drug Delivery Reviews* **2012**, 64, 246-255 DOI: 10.1016/j.addr.2012.09.022.
21. Ge, Z. S.; Liu, S. Y. Functional block copolymer assemblies responsive to tumor and intracellular microenvironments for site-specific drug delivery and enhanced imaging performance. *Chem. Soc. Rev.* **2013**, 42 (17), 7289-7325 DOI: 10.1039/c3cs60048c.
22. Okada, H.; Ogawa, T.; Tanaka, K.; Kanazawa, T.; Takashima, Y. Cytoplasm-responsive delivery systems for siRNA using cell-penetrating peptide nanomicelles. *Journal of Drug Delivery Science and Technology* **2014**, 24 (1), 3-11 DOI: 10.1016/s1773-2247(14)50001-9.
23. Abolmaali, S. S.; Tamaddon, A. M.; Salmanpour, M.; Mohammadi, S.; Dinarvand, R. Block ionomer micellar nanoparticles from double hydrophilic copolymers, classifications and promises for delivery of cancer chemotherapeutics. *European Journal of Pharmaceutical Sciences* **2017**, 104, 393-405 DOI: 10.1016/j.ejps.2017.04.009.
24. Chen, F.; Stenzel, M. H. Polyion Complex Micelles for Protein Delivery. *Austr. J. Chem.* **2018**, 71 (10), 768-780 DOI: 10.1071/ch18219.
25. Tiwari, S.; Bahadur, P. Modified hyaluronic acid based materials for biomedical applications. *International Journal of Biological Macromolecules* **2019**, 121, 556-571 DOI: 10.1016/j.ijbiomac.2018.10.049.
26. Lo, C. T.; Isawa, Y.; Nakabayashi, K.; Mori, H. Design of ion-conductive core-shell nanoparticles via site-selective quaternization of triazole triazolium salt block copolymers. *Eur. Polym. J.* **2018**, 105, 339-347 DOI: 10.1016/j.eurpolymj.2018.06.013.
27. Salamone, J. C.; Mahmud, M. U.; Watterson, A. C.; Olson, A. P.; Ellis, E. J. Polymerization of vinylpyridinium salts. 12. Occurrence of radical polymerization in spontaneous reactions. *J. Polym. Sci., Polym. Chem.* **1982**, 20 (5), 1153-1167 DOI: 10.1002/pol.1982.170200501.
28. Benjelloun, A.; Damas, C.; Brembilla, A.; Lochon, P. N-alkyl-3-vinylpyridinium salts - Homopolymerization of the hexadecyl derivative and behavior study of the polymer in aqueous media. *Polym. Bull.* **1994**, 33 (5), 513-520 DOI: 10.1007/bf00296158.
29. Navrotskii, A. V.; Novakov, I. A.; Zauer, E. A.; Orlyanskii, V. V.; Navrotskii, V. A. Kinetics of 1,2-dimethyl-5-vinylpyridinium methylsulfate polymerization initiated by tert-butylperoxypropanol. *Vysokomolekulyarnye Soedineniya Seriya a & Seriya B* **1999**, 41 (4), 589-594.
30. Navrotskii, A. V.; Makeev, S. M.; Orlyanskii, M. V.; Navrotskii, V. A.; Novakov, I. A. Specific features of 1,2-dimethyl-5-vinylpyridinium methyl sulfate polymerization in the presence of alpha-amino acids. *Polymer Science Series B* **2003**, 45 (7-8), 213-215.
31. Medjahed, K.; Tennouga, L.; Mansri, A. Series of Poly(4-vinylpyridine) Containing Quaternary Alkyl bromides: Synthesis and Determination Percentage of Quaternization. *Macromol. Symp.* **2014**, 339 (1), 130-133 DOI: 10.1002/masy.201300152.
32. Tennouga, L.; Bensalah, W.; Mansri, A. Poly(N-octyl-4-vinylpyridinium bromide) copolymers in aqueous solutions: potentiometric and thermodynamic studies. *E-Polymers* **2018**, 18 (6), 551-558 DOI: 10.1515/epoly-2018-0079.
33. Cecchini, M. M.; Steinkoenig, J.; Reale, S.; Barner, L.; Yuan, J.; Goldmann, A. S.; De Angelis, F.; Barner-Kowollik, C. Universal mass spectrometric analysis of poly(ionic liquid)s. *Chemical Science* **2016**, 7 (8), 4912-4921 DOI: 10.1039/c6sc01347c.
34. Convertine, A. J.; Sumerlin, B. S.; Thomas, D. B.; Lowe, A. B.; McCormick, C. L. Synthesis of block copolymers of 2- and 4-vinylpyridine by RAFT polymerization. *Macromolecules* **2003**, 36 (13), 4679-4681 DOI: 10.1021/ma034361l.
35. Bozovic-Vukic, J.; Manon, H. T.; Meuldijk, J.; Koning, C.; Klumperman, B. SAN-b-P4VP block copolymer synthesis by chain extension from RAFT-functional poly(4-vinylpyridine) in solution and in emulsion. *Macromolecules* **2007**, 40 (20), 7132-7139 DOI: 10.1021/ma070789z.
36. Wan, W.-M.; Pan, C.-Y. One-pot synthesis of polymeric nanomaterials via RAFT dispersion polymerization induced self-assembly and re-organization. *Polym. Chem.* **2010**, 1 (9), 1475-1484 DOI: 10.1039/c0py00124d.
37. Dong, S.; Zhao, W.; Lucien, F. P.; Perrier, S.; Zetterlund, P. B. Polymerization induced self-assembly: tuning of nano-object morphology by use of CO₂. *Polym. Chem.* **2015**, 6 (12), 2249-2254 DOI: 10.1039/c4py01632g.
38. Liu, H.; Ding, M.; Ding, Z.; Gao, C.; Zhang, W. In situ synthesis of the Ag/poly(4-vinylpyridine)block-polystyrene composite nanoparticles by dispersion RAFT polymerization. *Polym. Chem.* **2017**, 8 (20), 3203-3210 DOI: 10.1039/c7py00473g.
39. Zhang, W.-J.; Hong, C.-Y.; Pan, C.-Y. Fabrication of Spaced Concentric Vesicles and Polymerizations in RAFT Dispersion Polymerization. *Macromolecules* **2014**, 47 (5), 1664-1671 DOI: 10.1021/ma402497y.
40. Semsarilar, M.; Admiral, V.; Blanazs, A.; Armes, S. P. Anionic Polyelectrolyte-Stabilized Nanoparticles via RAFT Aqueous Dispersion Polymerization. *Langmuir* **2012**, 28 (1), 914-922 DOI: 10.1021/la203991y.
41. Chaduc, I.; Crepet, A.; Boyron, O.; Charleux, B.; D'Agosto, F.; Lansalot, M. Effect of the pH on the RAFT Polymerization of Acrylic Acid in Water. Application to the Synthesis of Poly(acrylic acid)-Stabilized Polystyrene Particles by RAFT Emulsion Polymerization. *Macromolecules* **2013**, 46 (15), 6013-6023 DOI: 10.1021/ma401070k.
42. Carlsson, L.; Fall, A.; Chaduc, I.; Wågberg, L.; Charleux, B.; Malmström, E.; D'Agosto, F.; Lansalot, M.; Carlmark, A. Modification of cellulose model surfaces by cationic polymer latexes prepared by RAFT-mediated surfactant-free emulsion polymerization. *Polym. Chem.* **2014**, 5, 6076-6086.
43. Semsarilar, M.; Admiral, V.; Blanazs, A.; Armes, S. P. Cationic Polyelectrolyte-Stabilized Nanoparticles via RAFT Aqueous Dispersion Polymerization. *Langmuir* **2013**, 29 (24), 7416-7424 DOI: 10.1021/la304279y.
44. Williams, M.; Penfold, N. J. W.; Armes, S. P. Cationic and reactive primary amine-stabilised nanoparticles via RAFT aqueous dispersion polymerisation. *Polym. Chem.* **2016**, 7 (2), 384-393 DOI: 10.1039/c5py01577d.
45. Zhang, B.; Yan, X.; Alcouffe, P.; Charlot, A.; Fleury, E.; Bernard, J. Aqueous RAFT Polymerization of Imidazolium-Type Ionic Liquid Monomers: En Route to Poly(ionic liquid)-Based Nanoparticles through RAFT Polymerization-Induced Self-Assembly. *ACS Macro Lett.* **2015**, 4 (9), 1008-1011 DOI: 10.1021/acsmacrolett.5b00534.
46. Fischer, A.; Brembilla, A.; Lochon, P. Synthesis of new amphiphilic cationic block copolymers and study of their behaviour in aqueous medium as regards hydrophobic microdomain formation. *Polymer* **2001**, 42 (4), 1441-1448 DOI: 10.1016/s0032-3861(00)00493-6.

47. Zamfir, M.; Patrickios, C. S.; Montagne, F.; Abetz, C.; Abetz, V.; Oss-Ronen, L.; Talmon, Y. Styrene-vinyl pyridine diblock copolymers: Synthesis by RAFT polymerization and self-assembly in solution and in the bulk. *J. Polym. Sci., Polym. Chem.* **2012**, *50* (8), 1636-1644 DOI: 10.1002/pola.25935.
48. Chen, A.; Blakey, I.; Whittaker, A. K.; Peng, H. The Influence of Casting Parameters on the Surface Morphology of PS-b-P4VP Honeycomb Films. *J. Polym. Sci., Polym. Chem.* **2016**, *54* (23), 3721-3732 DOI: 10.1002/pola.28268.
49. Derry, M. J.; Fielding, L. A.; Armes, S. P. Polymerization-induced self-assembly of block copolymer nanoparticles via RAFT non-aqueous dispersion polymerization. *Progr. Polym. Sci.* **2016**, *52*, 1-18 DOI: 10.1016/j.progpolymsci.2015.10.002.
50. Ponnusamy, K.; Babu, R. P.; Dhamodharan, R. Synthesis of block and graft copolymers of styrene by raft polymerization, using dodecyl-based trithiocarbonates as initiators and chain transfer agents. *J. Polym. Sci., Polym. Chem.* **2013**, *51* (5), 1066-1078 DOI: 10.1002/pola.26466.
51. Wan, W. M.; Pan, C. Y. Formation of Polymeric Yolk/Shell Nanomaterial by Polymerization-Induced Self-Assembly and Reorganization. *Macromolecules* **2010**, *43* (6), 2672-2675 DOI: 10.1021/ma100021a.
52. Zhang, Y.; Han, G.; Cao, M. J.; Guo, T. Y.; Zhang, W. Q. Influence of Solvophilic Homopolymers on RAFT Polymerization-Induced Self-Assembly. *Macromolecules* **2018**, *51* (11), 4397-4406 DOI: 10.1021/acs.macromol.8b00690.
53. Di Grandi, M. J.; Curran, K. J.; Baum, E. Z.; Bebernitz, G.; Ellestad, G. A.; Ding, W. D.; Lang, S. A.; Rossi, M.; Bloom, J. D. Pyrimido 1,2-b -1,2,4,5-tetrazin-6-ones as HCMV protease inhibitors: A new class of heterocycles with flavin-like redox properties. *Bioorganic & Medicinal Chemistry Letters* **2003**, *13* (20), 3483-3486 DOI: 10.1016/s0960-894x(03)00789-3.
54. Mai, Y. Y.; Eisenberg, A. Self-assembly of block copolymers. *Chem. Soc. Rev.* **2012**, *41* (18), 5969-5985 DOI: 10.1039/c2cs35115c.
55. Ferrari, R.; Lupi, M.; Colombo, C.; Morbidelli, M.; D'Incalci, M.; Moscatelli, D. Investigation of size, surface charge, PEGylation degree and concentration on the cellular uptake of polymer nanoparticles. *Colloids and Surfaces B-Biointerfaces* **2014**, *123*, 639-647 DOI: 10.1016/j.colsurfb.2014.10.003.
56. Chandrasiri, I.; Abebe, D. G.; Gupta, S.; Dal Williams, J. S.; Rieger, W. D.; Simms, B. L.; Yaddehige, M. L.; Noh, Y.; Payne, M. E.; Fortenberry, A. W.; Smith, A. E.; Ilavsky, J.; Grayson, S. M.; Schneider, G. J.; Watkins, D. L. Synthesis and characterization of polylactide-PAMAM "Janus-type" linear-dendritic hybrids. *J. Polym. Sci., Polym. Chem.* **2019**, *57* (13), 1448-1459 DOI: 10.1002/pola.29409.



Core cross-linked micelle (CCM)

Nanogel (NG)